

# Searches for Higgs Bosons beyond the Standard Model at the Tevatron Collider

F. Filthaut *for the CDF and D0 Collaborations*

*Radboud University and Nikhef, 6525 AJ Nijmegen, The Netherlands*

The rapidly increasing integrated luminosity collected by the CDF and D0 detectors at the Tevatron Collider has resulted in a wealth of new results from searches for Higgs bosons in the extensions of the Standard Model. Tighter limits are set on the parameters governing the Higgs sector in these models.

## 1. EXTENSIONS OF THE STANDARD MODEL HIGGS SECTOR

It is well known that the Standard Model (SM) of particle physics, successful as it is in describing the strong, electromagnetic, and weak interactions, cannot be complete. It does not allow for the incorporation of gravitation; and the mass of its scalar Higgs boson receives quadratic radiative corrections, making it unnatural for it to be as low as the order of the electroweak symmetry breaking scale, several hundred GeV.

The most popular extension of the SM designed to address these issues is Supersymmetry or SUSY. For each SM particle, it introduces a partner with spin differing by half a unit but with otherwise the same properties. This allows for a cancellation of radiative corrections due to loops of SM particles and their superpartners. But Supersymmetry must be broken, for otherwise the superpartners' masses would equal those of the SM particles, and SUSY would have long been discovered. The precise breaking mechanism depends on the interactions at energy scales inaccessible by the present-day colliders, and is not known.

A practical approach towards a description of SUSY phenomena at the energy scales accessible at experiments being conducted or in preparation is to consider the general *effective* theory obtained upon SUSY breaking: this is the Minimal Supersymmetric Standard Model (MSSM). Besides SUSY conserving interactions, it features *soft SUSY breaking* interactions that still maintain the cancellation of quadratic corrections to scalar masses, one of the reasons to introduce SUSY in the first place. The MSSM constructed in this fashion does have one severe drawback, however: it features 105 new and *a priori* arbitrary parameters. Even if many of these would give rise to unobserved features such as lepton flavour violation, and are hence constrained by measurements, the exploration of the full MSSM parameter space is a daunting task.

In contrast, the same Higgs sector that is at the root of the problems with the SM is described (at tree level) by a mere two parameters. SUSY requires the existence of two Higgs doublets (of hypercharge  $Y = 1$  and  $Y = -1$ ). Upon electroweak symmetry breaking, this results in five physical Higgs bosons: two charged ones,  $H^\pm$ , two CP-even neutral ones,  $h$  and  $H$  (by convention  $m_h < m_H$ ), and one CP-odd one,  $A$ . At tree level, all masses can be expressed as a function of only two parameters, usually taken to be  $m_A$  and the ratio of the two Higgs doublets' vacuum expectation values  $\tan\beta \equiv v_1/v_2$ .

Also the Higgs boson couplings to SM particles can be expressed as a function of  $m_A$  and  $\tan\beta$ . Table I shows the neutral Higgs boson couplings (here,  $\alpha$  is not a free parameter but itself depends on  $\tan\beta$  and  $m_A$ ); the  $H^\pm u_i d_j$  coupling is proportional to  $V_{u_i d_j} (m_{u_i} \cot\beta(1 - \gamma_5) + m_{d_j} \tan\beta(1 + \gamma_5))$ .

A remarkable feature is that (again at tree level)  $m_h < m_Z$ . This sole fact would be enough to exclude the MSSM, were it not for the fact that radiative corrections relax these constraints. In principle, these radiative corrections involve the whole MSSM, but the number of parameters contributing substantially is still small. As a general matter, a constraint  $m_h \lesssim 135\text{GeV}$  remains.

The radiative corrections affect the Higgs bosons' couplings as well as their masses. Rather than considering the

Table I: MSSM Neutral Higgs boson couplings to SM particles, relative to the respective SM Higgs boson couplings.

SM particle type	$h$ coupling	$H$ coupling	$A$ coupling
up-type quarks	$\frac{\cos \alpha}{\sin \beta}$	$\frac{\sin \alpha}{\sin \beta}$	$\cot \beta$
down-type quarks, $\ell^\pm$	$-\frac{\sin \alpha}{\cos \beta}$	$\frac{\cos \alpha}{\cos \beta}$	$\tan \beta$
W and Z bosons	$\sin(\beta - \alpha)$	$\cos(\beta - \alpha)$	0

whole MSSM parameter space, several representative *scenarios* are typically considered that evade the bounds set by searches for Higgs bosons conducted at the LEP  $e^+e^-$  Collider. Specifically, the scenarios considered here are  $m_h^{\max}$  scenario (with MSSM parameters tuned to obtain the highest possible  $m_h$ ) and the no-mixing scenario (with parameters tuned to switch off the mixing between the  $\tilde{t}_1$  and  $\tilde{t}_2$  superpartners of the top quark) [1]. Within these scenarios, the Higgsino mass parameter  $\mu$  is in principle fixed; however, given the sensitivity to this parameter, both  $\mu = +200\text{GeV}$  and  $\mu = -200\text{GeV}$  are considered in some of the analyses below.

## 2. NEUTRAL HIGGS BOSONS

### 2.1. Generalities

Previous searches at LEP for neutral Higgs bosons have excluded a large region of the  $(m_A, \tan \beta)$  parameter space where the lightest Higgs boson becomes sufficiently light to be accessible at LEP. In particular, the low  $\tan \beta$  region has been excluded up to large values of  $m_A$ .

The searches conducted at the Tevatron Collider are largely complementary to those earlier searches. At large values of  $\tan \beta$ , the enhanced couplings to  $b$  quarks and  $\tau$  leptons lead to significantly increased production cross sections. This fact, in combination with the particular signatures of  $b$ -quark jets and  $\tau$  leptons, is exploited below.

As a consequence of large  $\tan \beta$ , the masses of the  $A$  and  $H$  bosons (or  $A$  and  $h$ , for low values of  $m_A$ ) become almost degenerate (their mass difference becomes less than the corresponding detector resolution). This allows for a significant simplification in the analyses: rather than attempting to identify the two nearby resonances, they are simply lumped together, and denoted as  $\phi$  below. By comparison, the contribution from the “third” neutral Higgs boson becomes negligible.

### 2.2. $\phi \rightarrow b\bar{b}$

The  $b$  quark being the heaviest SM isospin  $-\frac{1}{2}$  fermion, the  $\phi \rightarrow b\bar{b}$  branching fraction is the largest one for high values of  $\tan \beta$ , becoming as high as  $\sim 0.9$ . As a consequence, it constitutes one of the dominant search channels. Unfortunately, this decay cannot be identified inclusively, due to an overwhelming QCD  $b\bar{b}$  production background. Instead, one looks for the final state in which the  $\phi$  is radiated off an initial state  $b$  quark<sup>1</sup>. A significant ( $\sim \tan^2 \beta$ ) cross section enhancement occurs also in this final state; the identification of a third  $b$  jet, typically of lower  $p_T$ , suppresses greatly the QCD background.

The CDF Collaboration has searched for the  $b\phi(\rightarrow b\bar{b})$  channel in a data sample corresponding to an integrated luminosity of  $1.9 \text{ fb}^{-1}$ , requiring all jets in a three-jet sample to be  $b$ -tagged by a displaced vertex algorithm [2].

Even this triple-tagged sample is dominated by QCD backgrounds. Each jet may be a genuine  $b$ -quark jet, or a fake (charm or light-flavour) jet. The two leading jets, hypothesized to result from the  $\phi$  decay, are treated on an equal footing. Therefore, considering only those final states containing at least two genuine  $b$ -quark jets leads to five background categories:  $bbb$ ,  $bbc$ ,  $bbq$ ,  $bcq$ , and  $bqb$  (here,  $q$  denotes a light-flavour jet).

<sup>1</sup>Here and in the following, charge conjugated final states are implied as well.

The distribution of the invariant mass  $m_{12}$  of the two leading jets for the signal is taken from simulation. For the backgrounds no adequate simulation exists, and templates for each of the above categories are obtained starting from a data sample containing at least two  $b$  tags. For the first three categories, this starts from a  $bbj$  sample to which parametrized efficiencies for tagging the third jet ( $b$ ,  $c$ , or  $q$ ) are applied; for the  $bqb$  category, a similar procedure is applied to events with the third and one of the two leading jets already tagged. An additional correction, derived from simulation, is applied to account for the different processes contributing to final states with more than two  $b$  jets. Finally, the  $bcb$  distribution is assumed to look like the  $bbb$  one, but with only a subset of processes contributing; another simulation-derived correction is applied to account for this.

The normalization of the distributions obtained in this fashion are adjusted to fit the data distribution. However, as can be observed from Fig. 1, some of the background templates cannot be distinguished. Therefore, a second variable involving the vertex masses (the invariant mass of all tracks, assuming they are  $\pi^\pm$ , attached to the displaced vertices) is constructed. This is done starting from the same data samples above, and uses the same information in addition to known vertex mass distributions for different flavours.

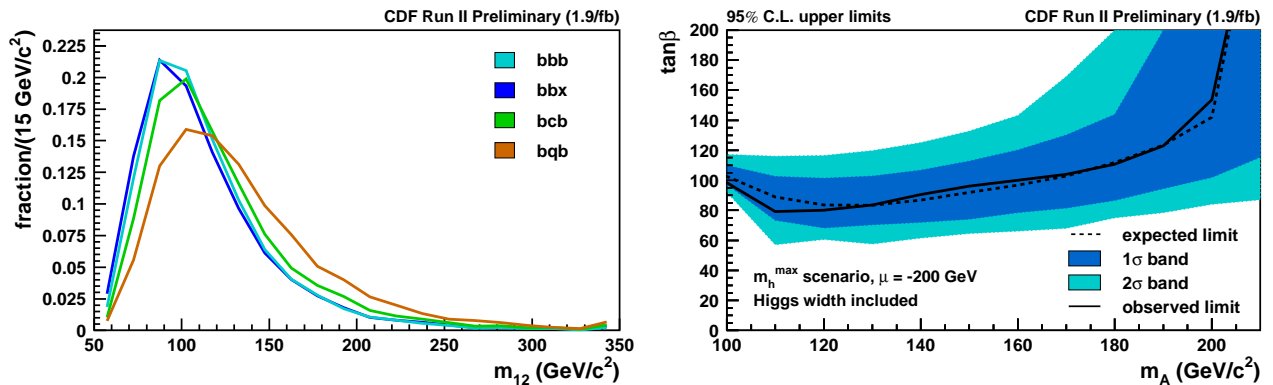


Figure 1: Left: invariant mass distributions for various background sources in the CDF  $\phi \rightarrow b\bar{b}$  analysis. Right: limits in the  $(m_A, \tan\beta)$  plane in the  $m_h^{\max}$  scenario.

For each hypothesized value of  $m_\phi$ , two template fits are then carried out jointly to the two distributions, one with and one without the assumed signal. No significant improvement in the fit likelihood is observed upon inclusion of a signal component; limits on a possible signal component are set in a modified frequentist framework based on [3].

A complication is that for sufficiently high values of  $\tan\beta$ , the neutral Higgs boson decay width exceeds the experimental invariant mass resolution. The resulting broadening of the signal  $m_{12}$  distribution reduces the discrimination power between signal and backgrounds, and needs to be taken into account explicitly.

A similar analysis has been carried out by the D0 Collaboration on a  $1 \text{ fb}^{-1}$  dataset [4]. An artificial neural network  $b$ -tagging algorithm exploiting lifetime information was employed. Rather than using a second discriminating variable to determine the various background components, multiple  $b$ -tagging criteria (with known efficiencies) are used to determine the composition of the double-tagged sample.

A second discriminating variable, based on kinematic information, is subsequently used nevertheless, to suppress further the QCD backgrounds. Two discriminants  $D$  are constructed, one combining low-mass (90–130 GeV) and one combining high-mass (130–220 GeV) simulated Higgs signal samples. The background predictions are obtained, as a function of both the invariant mass and the discriminant, by applying a correction derived from simulation to the double-tagged sample. Fig. 2 compares the low-mass discriminant distribution integrated over all invariant masses, with its prediction; a good agreement is observed for the background dominated low- $D$  region. The final background predictions are obtained by selecting the high- $D$  region. The whole analysis is applied jointly to exclusive three-, four-, and five-jet data samples. Again no significant excess of data over predictions is observed, and a modified frequentist method based on [3] is used to set limits on a possible signal. The results are also shown for both the no-mixing and  $m_h^{\max}$  scenarios in Fig. 2. A slight excess, not enough to be qualified as a signal, is observed at masses

between 150 and 200 GeV, leading to a reduced exclusion region compared to the predictions.

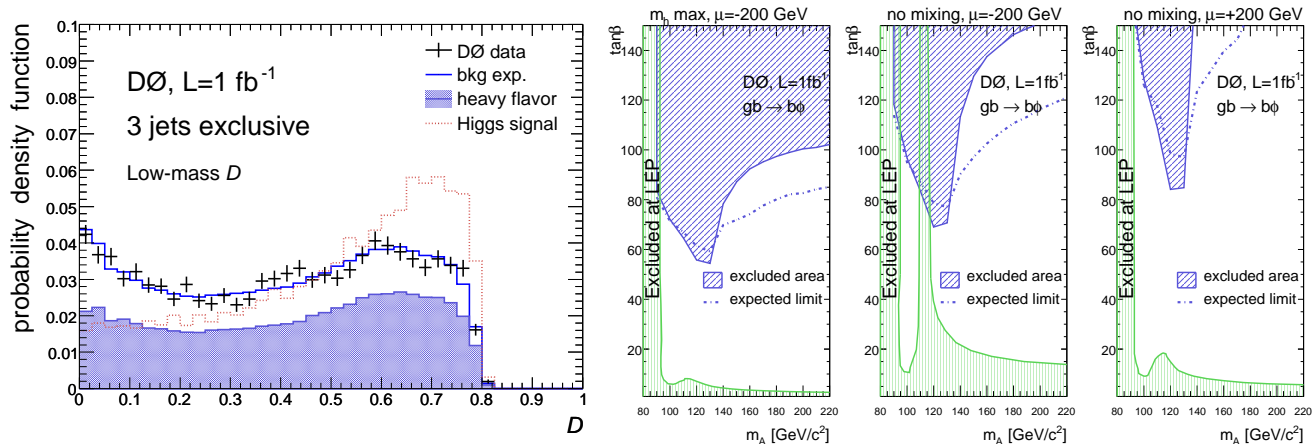


Figure 2: Left: low-mass kinematic discriminant distribution in the  $D0 \phi \rightarrow bb$  analysis. Right: limits in the  $(m_A, \tan\beta)$  plane in different scenarios.

### 2.3. $\phi \rightarrow \tau^+\tau^-$

For high  $\tan\beta$ , the branching fraction for the decay  $\phi \rightarrow \tau^+\tau^-$  is approximately 0.1. The drawback of this lower branching fraction is offset, however, by the absence of irreducible QCD background. The relative cleanliness of this decay channel allows for an inclusive analysis, where the  $\phi$  can be produced singly, through gluon fusion  $gg \rightarrow \phi$ .

A new  $D0$  analysis has been performed on  $e\tau_h$ ,  $\mu\tau_h$ , and  $e\mu$  final states (here, only the  $\tau$  decay products are indicated and neutrinos omitted;  $\tau_h$  indicates the  $\tau$  hadronic decay mode) in a  $1 \text{ fb}^{-1}$  dataset [5]. Hadronic  $\tau$  decays are classified according to their charged track and EM cluster multiplicities, and are selected efficiently using artificial neural networks.

The signal is characterized by two high- $p_T$   $\tau$  leptons. To reject  $W(\rightarrow \ell\nu)$ +jets events with a jet misidentified as a  $\tau_h$ , the transverse mass reconstructed from lepton and the missing transverse momentum vector (interpreted as a single neutrino) must be below 40 GeV in the  $\mu\tau_h$  channel and 50 GeV in the  $e\tau_h$  channel. Backgrounds from  $t\bar{t}$  events are suppressed by vetoing events with high jet activity.

The irreducible background from  $Z \rightarrow \tau^+\tau^-$  remains and is estimated using simulation. Signal events are recognized as an excess over background predictions in the distribution of the *visible mass*  $m_{\text{vis}}$ , computed as the invariant mass of the visible  $\tau$  decay products and the missing momentum four-vector approximated as  $\not{p} \equiv \left(\sqrt{\not{E}_x^2 + \not{E}_y^2}, \not{E}_x, \not{E}_y, 0\right)$ .

The visible mass distribution is shown in Fig. 3 for the three channels considered. The expected signal due to a 160 GeV Higgs boson is also indicated. No significant excess is observed, and limits are again set using the modified frequentist framework. It should be pointed out that here, due to the worse experimental resolution caused by the escaping neutrinos, the effects of the finite  $\phi$  decay width are very modest.

A very similar CDF analysis has been carried out on a  $1.8 \text{ fb}^{-1}$  dataset [6]. An earlier analysis, performed on  $1 \text{ fb}^{-1}$ , yielded a small excess that could be attributed to a Higgs boson of mass  $m_\phi \approx 140 \text{ GeV}$ . With the increased statistics considered here, a good overall agreement between data and background predictions is obtained. This analysis now sets the tightest limits in the  $(m_A, \tan\beta)$  plane, as displayed in Fig. 4.

### 2.4. Fermiophobic Higgs Bosons

Besides the reasonably “standard” no-mixing and  $m_h^{\text{max}}$  scenarios, alternative scenarios are possible where the Higgs boson couplings to fermions are small; an example is the “small  $\alpha_{\text{eff}}$ ” scenario [1], in which radiative corrections

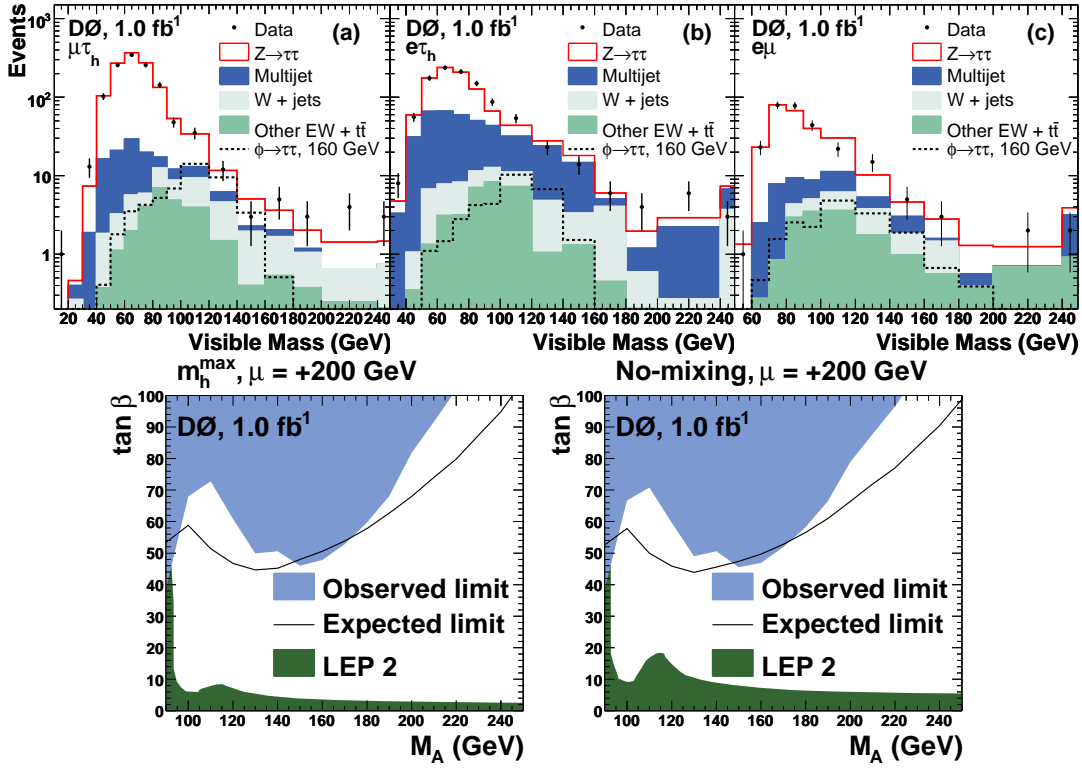


Figure 3: Top: visible mass distribution in the three channels considered in the D0  $\phi \rightarrow \tau^+\tau^-$  search. Bottom: limits in the  $(m_A, \tan\beta)$  plane obtained in the  $m_h^{\text{max}}$  (left) and no-mixing scenarios.

conspire to yield small effective couplings to down-type quarks and charged leptons.

The D0 Collaboration has considered a *fermiophobic* Higgs model, in which all couplings to fermions are suppressed but the couplings to gauge bosons are unmodified. In a  $2.3 \text{ fb}^{-1}$  dataset, a search was performed for the decay  $h \rightarrow \gamma\gamma$  [7]. This would be the main decay mode for relatively light Higgs bosons,  $m_h \lesssim 100 \text{ GeV}$ .

Backgrounds to this process originate from QCD direct  $\gamma\gamma$  events, as well as  $\gamma$ +jet and di-jet events in which one or both jets, respectively, are mis-identified as photons. The mis-identification contribution is suppressed using a neural network employing variables based on calorimeter shower shapes; the network performance has been measured in  $Z \rightarrow e^+e^-$  events and samples of photon-like QCD jets. Starting from a loose preselection, the identification of events where neither, one, or two of the photon candidates satisfy a tight neural network cut allows to determine the contributions from the individual backgrounds. The irreducible  $\gamma\gamma$  background estimated in this way is consistent with the result obtained from a NLO calculation. The contribution from  $Z \rightarrow e^+e^-$  events where both electrons are identified as photons, is estimated from simulation.

The  $\gamma\gamma$  invariant mass distribution is shown in Fig. 5, along with the signal of a 130 GeV Higgs boson. No excess over predictions is observed, and limits are set on the possible cross section for the production of such events. The limits are also shown in Fig. 5.

For higher values of  $m_h$ , the  $h \rightarrow W^+W^-$  decay mode becomes dominant. The CDF Collaboration has exploited this by using a SM Higgs boson search in the channel  $W^\pm h \rightarrow W^\pm W^+W^-$  in a  $1.9 \text{ fb}^{-1}$  dataset, and interpreting its result in the context of a search for fermiophobic Higgs bosons [8]. The main difference with the corresponding SM search is that the branching fraction for this Higgs boson decay mode is relatively high even for lower values of  $m_h$ .

The requirement of two isolated leptons of the same charge sign results in a nearly background free sample. The remaining backgrounds are due to fake leptons and their rate, after the requirement of isolated tracks with certain energy deposits in the hadron calorimeters, is estimated from inclusive jet samples. No signal is observed in the distributions of relevant kinematic variables (see *e.g.* Fig. 6), and also the cross section limits obtained are compared

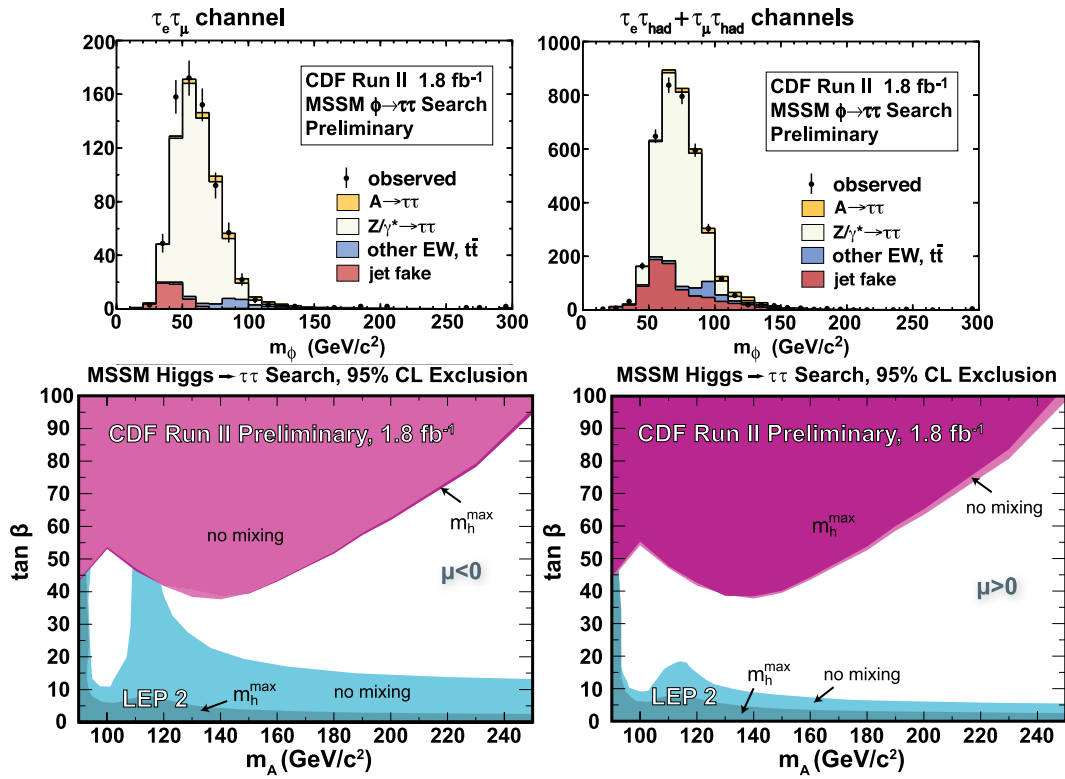


Figure 4: Top: visible mass distribution in the  $e\mu$  channel (left) and in the  $e\tau_h + \mu\tau_h$  channels (right) in the CDF  $\phi \rightarrow \tau^+\tau^-$  search. Bottom: limits in the  $(m_A, \tan\beta)$  plane, for  $\mu < 0$  (left) and  $\mu > 0$  (right).

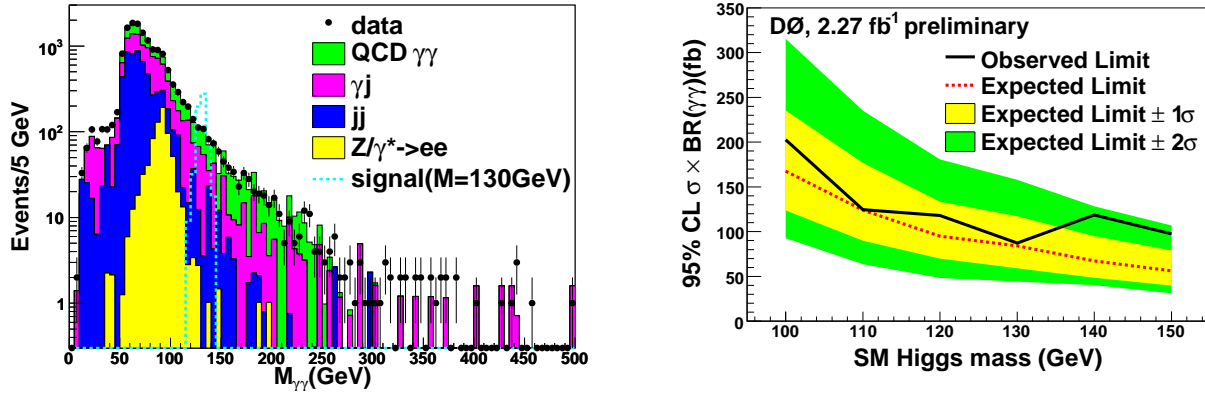


Figure 5: Left:  $\gamma\gamma$  invariant mass distribution in the D0  $h \rightarrow \gamma\gamma$  search. Right: cross section limit as a function of  $m_h$ .

with predictions for SM and fermiophobic Higgs boson production in Fig. 6.

### 3. CHARGED HIGGS BOSONS

Charged Higgs bosons have previously been searched for at the LEP Collider, in their decays to  $\tau\bar{\nu}$  or  $c\bar{s}$  final states. Assuming that these two decay modes saturate the  $H^\pm$  decays, masses below 79 GeV were excluded.

If  $H^\pm$  are relatively light,  $m(H^\pm) < m_t - m_b$ , their dominant production mechanism at the Tevatron collider is in decays of top quarks,  $t \rightarrow bH^+$ . This decay mode may be an important one either at low or at high values of  $\tan\beta$  (due to the  $m_t \cot\beta$  and  $m_b \tan\beta$  terms in the coupling, respectively). For moderate to high  $\tan\beta$  it decays

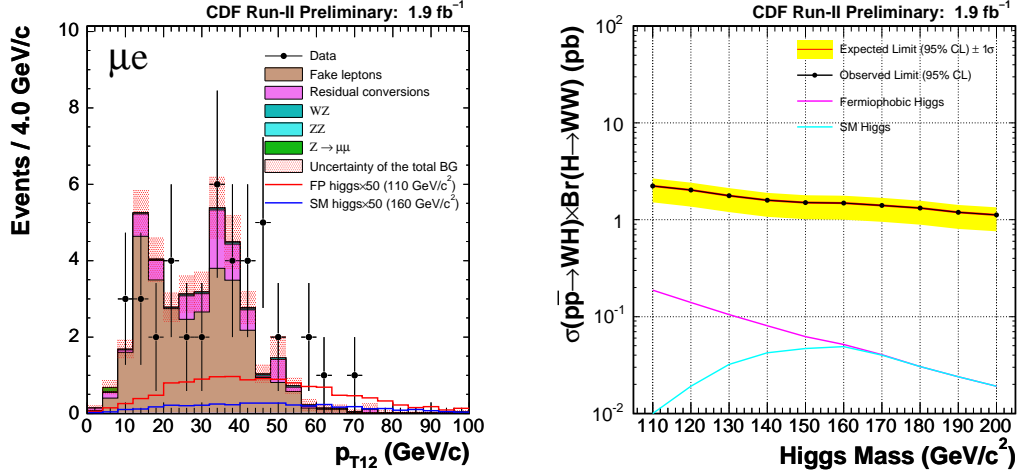


Figure 6: Left: transverse momentum of the dilepton system for the  $\mu^\pm e^\mp$  channel in the CDF  $Wh \rightarrow WWW$  search. Right: resulting cross section limits as a function of  $m_h$ , compared with the predictions for SM and fermiophobic Higgs boson production.

primarily to  $\tau\bar{\nu}$ , while for low values the decay is mostly to  $c\bar{s}$ .

The D0 Collaboration has re-interpreted existing  $t\bar{t}$  production cross section measurements in the context of a search for the decay  $H^\pm \rightarrow c\bar{s}$  under the pessimistic assumption that  $m(H^\pm) \approx m_W$  [9]. The only observable consequence of such a scenario is an apparent increased branching fraction for hadronic decays of the  $W$  boson; this can be tested by a comparison of the measured di-lepton and  $\ell$ +jets  $t\bar{t}$  cross sections. From the observed ratio,  $\sigma(p\bar{p} \rightarrow t\bar{t})_{\ell+jets} / \sigma(p\bar{p} \rightarrow t\bar{t})_{\ell\ell} = 1.21_{-0.26}^{+0.27}$ , application of the Feldman-Cousins likelihood ordering principle [10] leads to the result  $B(t \rightarrow H^\pm b) < 0.35$  at 95% CL.

A new CDF analysis, on a  $2.2 \text{ fb}^{-1}$  dataset, has been carried out looking for the same decay but under the assumption that  $m(H^\pm) > M_W$  [11]. The analysis is restricted to  $\ell$ +jets  $t\bar{t}$  candidate events, requiring in addition four jets in the final state, two of which must be  $b$  tagged.

The invariant mass of the remaining two jets is computed. Neglecting backgrounds and resolution effects, the resulting distribution should yield the  $W$  boson mass. If part of the decays are to charged Higgs bosons, the invariant mass distribution is modified. A comparison between measured and predicted invariant mass distributions is shown in Fig. 7, with in addition the expected upper limit at 95% CL for the signal of a putative charged Higgs boson of mass 120 GeV. No such deformation of the di-jet invariant mass distribution is observed, and upper limits on  $B(t \rightarrow H^\pm b) \cdot B(H^\pm \rightarrow c\bar{s})$  are also given in Fig. 7.

## 4. DOUBLY CHARGED HIGGS BOSONS

A more exotic extension of the SM Higgs sector is to posit the existence of Higgs multiplets with weak isospin  $I > \frac{1}{2}$ , leading to doubly charged Higgs bosons  $H^{\pm\pm}$ . In general, such extensions are severely constrained by the  $\rho$  parameter, which is  $\rho \equiv m_W^2 / m_Z^2 \cos^2 \theta_W = 1$  at tree level if only Higgs doublets are present but can be altered significantly in the presence of  $I > \frac{1}{2}$  multiplets. However, these constraints can be evaded if the doubly charged Higgs boson coupling to  $W$  bosons vanishes. Two models exist, with “left-handed” (“right-handed”) Higgs bosons coupling to left-handed (right-handed) fermions, respectively.

The D0 Collaboration has searched in a  $1.1 \text{ fb}^{-1}$  dataset for such doubly charged Higgs bosons produced through the process  $p\bar{p} \rightarrow Z/\gamma^* \rightarrow H^{++}H^{--}$ , with both Higgs bosons decaying to muons,  $H^{\pm\pm} \rightarrow \mu^\pm\mu^\pm$  [12]. As in the case of the CDF search for fermiophobic Higgs bosons (see Sect. 2.4), a clean sample is obtained by the requirement of

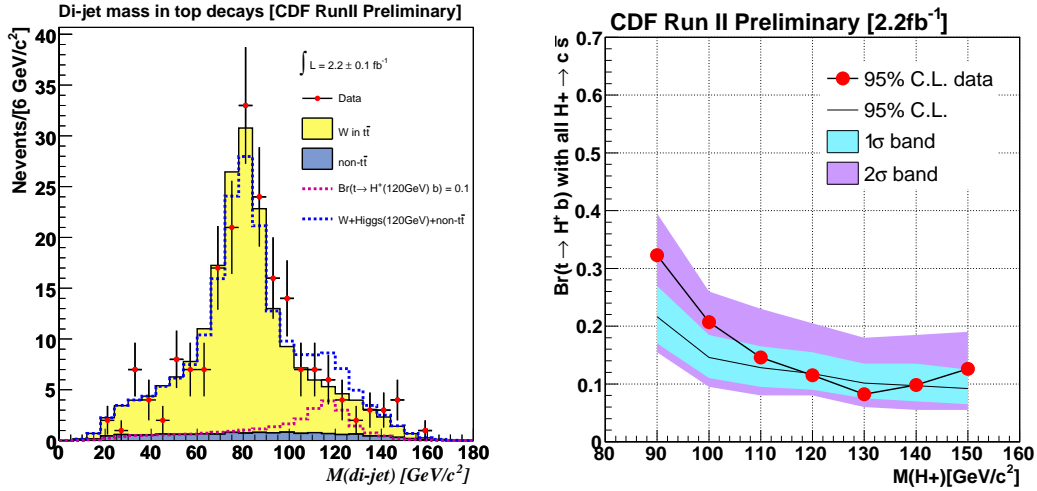


Figure 7: Left: di-jet invariant mass in the CDF  $t \rightarrow H^+b$ ,  $H^+ \rightarrow c\bar{s}$  search. The expected deformation due to a 120 GeV  $H^\pm$  is also shown, for the purpose of illustration. Right: resulting upper limits on the product of branching fractions  $B(t \rightarrow H^+b) \cdot B(H^+ \rightarrow c\bar{s})$ .

two like-sign isolated muons. Further sensitivity is achieved by requiring a third muon to be present. The dominant background is from  $WZ$  and  $ZZ$  events, with muons associated with a jet passing the isolation criteria. The isolation fake rate is known and is applied to scale these backgrounds, inferred from simulation. The number of heavy flavour events (with again muons resulting from semi-muonic decays appearing to be isolated) is estimated from the number of such events with opposite charge sign.

Three events remain after all selection criteria, consistent with background expectations as shown in Fig. 8. The resulting cross-section limit, obtained as a function of the Higgs boson mass, is compared with the theoretical cross-section. This is similarly shown in Fig. 8. Lower limits of 150 GeV(127 GeV) for left-handed (right-handed) doubly charged Higgs bosons are obtained.

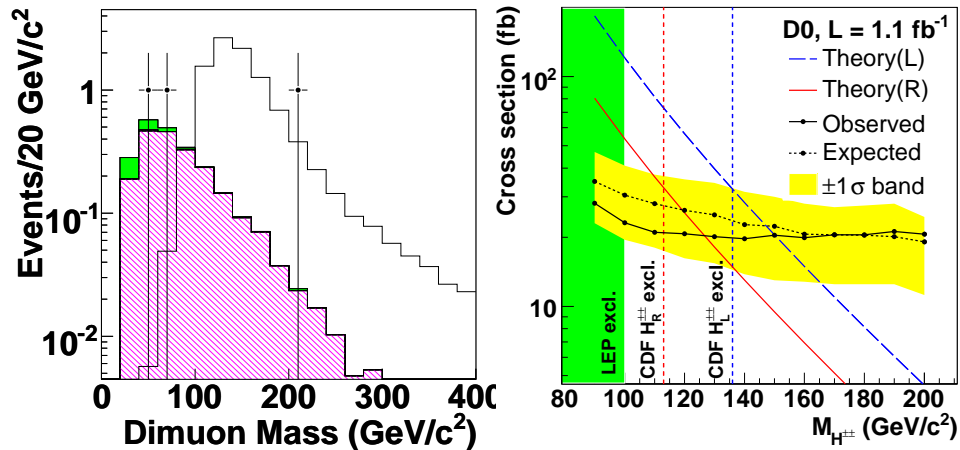


Figure 8: Left: like-sign di-muon invariant mass after all selection criteria in the D0 search for doubly charged Higgs bosons. The dark- and light-hatched areas represent the expected multi-jet and  $WZ/ZZ$  backgrounds; the open histogram represents the expected signal due to a left-handed  $H^{\pm\pm}$  with a mass of 140 GeV. Right: resulting cross section limits as a function of the doubly charged Higgs boson mass.



## References

- [1] M. Carena, S. Heinemeyer, C.E.M. Wagner, and G. Weiglein, “Suggestions for benchmark scenarios for MSSM Higgs boson searches at hadron colliders”, *Eur. Phys. J. C* **26** (2003) 601; M. Carena, S. Heinemeyer, C.E.M. Wagner, and G. Weiglein, “MSSM Higgs Boson Searches at the Tevatron and the LHC: Impact of Different Benchmark Scenarios”, *Eur. Phys. J. C* **45** (2006) 797.
- [2] CDF Collaboration, “Search for Higgs Bosons Produced in Association with  $b$ -Quarks”, CDF Note 9284, [http://www-cdf.fnal.gov/physics/new/hdg/results/3b\\_susyhiggs\\_080229/](http://www-cdf.fnal.gov/physics/new/hdg/results/3b_susyhiggs_080229/), 2008.
- [3] T. Junk, “Confidence level computation for combining searches with small statistics”, *Nucl. Instrum. Meth.* **A434** (1999) 435; A. Read, “Linear interpolation of histograms”, *Nucl. Instrum. Meth.* **A425** (1999) 357.
- [4] D0 Collaboration, Search for neutral Higgs bosons in multi- $b$ -jet events in  $p\bar{p}$  collisions at  $\sqrt{s} = 1.96\text{TeV}$ , arXiv:0805.3556 [hep-ex], submitted to *Phys. Rev. Lett.*
- [5] D0 Collaboration, “Search for Higgs bosons decaying to tau pairs in  $p\bar{p}$  collisions with the D0 detector”, arXiv:0805.2491 [hep-ex], accepted by *Phys. Rev. Lett.*
- [6] CDF Collaboration, “Search for Neutral MSSM Higgs Bosons Decaying to Tau Pairs”, CDF Note 9071, [http://www-cdf.fnal.gov/physics/new/hdg/results/htt\\_070928/](http://www-cdf.fnal.gov/physics/new/hdg/results/htt_070928/), 2008.
- [7] D0 Collaboration, “Search for a light Higgs boson in  $\gamma\gamma$  final states at D0”, D0 Note 5601-CONF, <http://www-d0.fnal.gov/Run2Physics/WWW/results/prelim/HIGGS/H48/H48.pdf>, 2008.
- [8] CDF Collaboration, “Search for the  $Wh$  Production Using High- $p_T$  Isolated Like-Sign Dilepton Events in Run-II”, CDF Note 7307, [http://www-cdf.fnal.gov/physics/new/hdg/results/whwww\\_080411/](http://www-cdf.fnal.gov/physics/new/hdg/results/whwww_080411/), 2008.
- [9] D0 Collaboration, “Measurement of the Cross Section Ratio  $\sigma(p\bar{p} \rightarrow t\bar{t})_{\ell+jets}/\sigma(p\bar{p} \rightarrow t\bar{t})_{\ell\ell}$  with the D0 Detector at  $\sqrt{s} = 1.96\text{TeV}$  in the Run II Data”, D0 Note 5466-CONF, <http://www-d0.fnal.gov/Run2Physics/WWW/results/prelim/TOP/T61/T61.pdf>, 2008.
- [10] G.J. Feldman and R.D. Cousins, “A Unified approach to the classical statistical analysis of small signals”, *Phys. Rev. D* **57** (1998) 3873.
- [11] CDF Collaboration, “A search for charged Higgs in lepton+jets  $t\bar{t}$  events using 2.2  $\text{fb}^{-1}$  of CDF data”, CDF Note 9322, [http://www-cdf.fnal.gov/physics/new/top/2008/tprop/ChargedHiggs/chiggs\\_pub.html](http://www-cdf.fnal.gov/physics/new/top/2008/tprop/ChargedHiggs/chiggs_pub.html), 2008.
- [12] D0 Collaboration, “Search for Pair Production of Doubly-charged Higgs Bosons in the  $H^{++}H^{--} \rightarrow \mu^+\mu^+\mu^-\mu^-$  Final State at D0”, arXiv:0803.1534 [hep-ex], accepted by *Phys. Rev. Lett.*